Filamentous recombinant human Tau activates primary astrocytes via an integrin receptor complex

Peng Wang[1], Yihong Ye[1]*

[1] Laboratory of Molecular Biology, National Institute of Diabetes and Digestive and Kidney Diseases, National Institutes of Health, Bethesda, MD 20892

Correspondence should be sent to:

Yihong Ye

email: yihongy@mail.nih.gov

Tel: 301-594-0845

Fax: 301-496-0201

ORCID ID# 0000-0002-9512-7922

Running title: αV/β1 integrin is a Tau receptor in astrocytes

Key words: Tau, Tauopathy, Alzheimer's disease/AD, misfolded proteins, endocytosis, integrin αV/β1 (ITGαV/β1), integrin signaling, astrocyte activation, neuroinflammation

Microtubule-associated protein Tau can form protein aggregates transmissible within the brain, correlating with the progression of tauopathies in humans. The transmission of aggregates requires neuron-released Tau to interact with surface receptors on target cells. However, the underlying molecular mechanisms in astrocytes and downstream effects are unclear. Here, using a spatially resolved proteomic mapping strategy, we show that integrin αV/β1 receptor binds recombinant human Tau, mediating the entry of Tau fibrils in astrocytes. The binding of distinct Tau species to the astrocytic αV/β1 receptor differentially activate integrin signaling. Furthermore, Tau-mediated activation of integrin signaling results in NFκB activation, causing upregulation of pro-inflammatory cytokines and chemokines, induction of a sub-group of neurotoxic astrocytic markers, and release of neurotoxic factors. Our findings suggest that filamentous recombinant human Tau-mediated activation of integrin signaling induces astrocyte conversion towards a neurotoxic state, providing a mechanistic insight into tauopathies.

Clinically documented protein aggregates such as extracellular amyloid plaques and intracellular neurofibrillary tangles (NFTs) are pathological hallmarks of neurodegenerative diseases such as Alzheimer's disease (AD). NFTs are formed primarily by hyper-phosphorylated Tau, a soluble microtubule-binding protein abundantly expressed in neurons of the central nervous system (CNS) [1, 2]. The primary function of Tau is to stabilize microtubules, but its intrinsic misfolding propensity prompts it to form toxic filamentous aggregates, particularly in neurons during aging. In addition to AD, Tau-containing NFTs have been linked to brain dysfunctions in other neurodegenerative diseases such as Pick's disease and frontotemporal dementia, which are collectively termed Tauopathies [1].

An unusual characteristic of tauopathies is the prion-like propagation of Tau-containing aggregates, which seems to correlate with the decline of cognition during disease progression [1-6]. This protein propagation process may involve the release of Tau in either monomeric or aggregated forms, followed by the uptake by recipient cells (neurons or glial cells) [7]. Tau fibrils formed along this path can serve as 'seeds' once inside a target cell, converting endogenous Tau monomers into an aggregation-prone toxic conformer. Accumulating evidence suggests that both monomeric Tau and Tau aggregates can be released from neurons independent of cell death, and this process is enhanced by neuronal activities [8-10]. The mechanisms underlying Tau release are controversial. Specifically, some studies showed that Tau is predominantly released in a free soluble form [11-14] but a study suggested membrane-associated vesicles as a major extracellular Tau carrier [8]. By contrast, numerous studies showed that neurons, microglia, and

astrocytes all could readily internalize different Tau species [15-18]. In certain immortalized cells, endocytosis of Tau preformed fibrils (PFFs) is initiated when Tau binds to heparan sulfate proteoglycans (HSPGs) on the cell surface [19-21], which cooperate with a membrane receptor to mediate Tau internalization [22], but other unidentified mechanisms also contribute to Tau uptake, particularly in primary non-neuronal cells [22, 23].

In addition to damaging endogenous Tau folding when Tau PFFs enter neurons, Tau fibrils can also influence non-neuronal cells from the cell exterior. This model is particularly attractive in the complex brain microenvironment in which the fitness of neurons is tightly modulated by glial cells such as astrocytes [24, 25]. It was shown that the activation of astrocytes by lipopolysaccharide (LPS) can alter their phagocytic activity, which might mitigate Tauopathies as activated astrocytes help to clear protein aggregates [26, 27]. However, activated astrocytes might also exacerbate Tauopathies because they can contribute to neuroinflammation by releasing pro-inflammatory cytokines and chemokines [28, 29]. Notably, a recent transcription profiling study revealed two distinct functional states of reactive astrocytes termed as “A1” and “A2”, respectively [30]. A2 astrocytes appear to restore neuronal activities after injury, whereas A1 astrocytes not only fail to promote synapse formation, but also gain a neurotoxic activity by releasing some unknown factors.

How astrocytes are converted to a neurotoxic state is a key question relevant to many neurodegenerative diseases. To date, accumulating evidence suggest that microglia activated during the classic inflammation response can serve as an essential mediator of astrocytic A1 conversion because factors released by reactive microglia are sufficient to

activate the astrocyte A1 state [30]. However, whether neurotoxic astrocytes can be induced independent of microglia under stress or disease conditions is unknown.

Given the close link between Tau misfolding and neurodegenerative diseases, we] investigate whether harmful insults triggered by extracellular Tau aggregates can directly convert astrocytes to a neurotoxic state. We used a proximity-based ligation approach to identify the αV/β1 integrin complex as a receptor for Tau monomer and fibrils in primary astrocytes. The ligation of Tau fibrils to integrin not only initiates their internalization, but also activates integrin signaling, which in turn induces inflammation and converts astrocytes into an A1-like neurotoxic state. These findings establish a direct link between misfolding-associated proteotoxic stress and astrocyte activation.

Results

HSPG-independent uptake of Tau PFFs by primary astrocytes

To study the mechanism of Tau fibril uptake in primary astrocytes, we purified Tau (2N4R) as a recombinant protein from *E. coli* (Supplementary Fig. 1a) and labeled it with a fluorescent dye ($Alexa_{594}$). We used the labeled protein to generate PFFs following a well-established protocol (Supplementary Fig. 1b) [31], and then treated mouse primary astrocytes with labeled monomeric Tau or PFFs. Incubating astrocytes with Tau for up to 6 h did not cause detectable cell death (Supplementary Fig. 1c) but led to efficient internalization of Tau PFFs. Unlike immortalized cell lines, Tau PFF uptake by primary astrocytes was largely unaffected by heparin (Supplementary Fig. 1d, e), a competitive inhibitor that blocks Tau PFF binding to HSPGs in some cell lines [19-21]. This result is in line

with another study, which suggests that primary astrocytes do not use HSPGs for Tau PFF internalization [32]. Instead, an unknown Tau receptor(s) is involved.

Identification of integrin αV/β1 as a Tau interactor in primary astrocytes

Because Tau monomers could also enter primary astrocytes, albeit with reduced efficiency compared to Tau PFFs [15, 32], we presumed that Tau fibrils and monomers engaged a common receptor but with different affinities. Therefore, we employed a proximity labeling-based proteomic mapping strategy using purified APEX2-tagged Tau monomer as the bait (Figure 1a). APEX2 is an engineered peroxidase that can covalently tag proximal lysine side chains with biotin molecules in the presence of biotin-phenoxyl radicals [33]. Because the relatively large APEX2 fusion might affect the interaction of Tau with the plasma membrane, we first used Sh-SY5Y cells to characterize the membrane interaction of Tau fusion proteins (Figure 1b). When APEX2 was fused to the C-terminus of Tau, Tau-APEX2 bound efficiently to the cell surface in a dose dependent manner, but the addition of APEX2 to the N-terminus abolished the binding (Supplementary Fig. 2a, b). Thus, consistent with previous reports [34, 35], Tau binding to the plasma membrane is mediated by a sequence near the N-terminus, which can be masked by a proximal APEX2 fusion.

To identify Tau receptor, we incubated Tau-APEX2 or APEX2 as a control with primary astrocytes at 4 °C for 30 min to allow membrane binding. This short incubation did not affect membrane permeability or induce cell death (Supplementary Fig. 2c). We then performed biotin labeling and the labelled plasma membrane proteins were enriched

by streptavidin-affinity purification. Immunoblotting using biotin antibodies detected a major biotinylation product with Mr. of ~120kDa (Figure 1c). As expected, APEX2 alone was not able to biotinylate this 120kDa protein (Figure 1c). Mass spectrometry analysis of the excised band identified several membrane proteins enriched in Tau-APEX2-treated cells (Supplementary Fig. 2d). Interestingly, the top candidates were all cell adhesion molecules such as integrins and neural cell adhesion molecules (NCAM).

The identification of integrin as a potential Tau receptor was intriguing given that genetic variations in integrin genes had been suggested as a potential risk factor for neuroinflammation/neurodegeneration [36-38] and that α6/β1 integrin was shown to facilitate phagocytosis-mediated elimination of Aβ amyloid [39, 40]. Since αV/β1 integrin (ITGαV/β1) was the most significantly modified proteins (based on peptide count), we focused this study on ITGαV/β1.

To validate the interaction of Tau-APEX2 with αV/β1 integrin, we repeated Tau-APEX2-mediated biotinylation using HEK293T cells over-expressing either Flag-tagged ITGαV or GFP-tagged ITGβ1. Following cell surface biotinylation and streptavidin pulldown, these proteins could be detected by immunoblotting using antibodies recognizing their corresponding tags (Figure 1d, Supplementary Fig. 2e), suggesting that they could indeed be biotinylated by Tau-APEX2. Similar experiments performed in primary astrocytes further confirmed that endogenous ITGαV/β1 could be biotinylated by Tau-APEX2 but not APEX2 (Figure 1e). Importantly, after Tau-APEX2 binding to the cell surface, immunoprecipitation of Tau-APEX2 from cell extracts using a Tau specific

antibody also co-precipitated endogenous ITGαV/β1 (Figure 1f). Likewise, when Tau-APEX2 was incubated with purified ITGαV/β1 ectodomains, immunoprecipitation of Tau also co-precipitated ITGαV/β1 (Supplementary Fig. 3a). Thus, the biotinylation of ITGαV/β1 by Tau-APEX2 is likely a result of a direct interaction between these proteins.

αV/β1 integrin mediates Tau PFF uptake in primary astrocytes

We next tested whether Tau PFFs also interacted with endogenous ITGαV/β1 by co-immunoprecipitation. To this end, we incubated primary astrocytes in the presence or absence of Tau PFFs on ice before solubilizing cells by a NP40-containing buffer. Immunoprecipitation using Tau antibodies precipitated Tau PFFs together with a fraction of endogenous ITGαV/β1 (Figure 2A, lane 9). By contrast, ITGαV/β1 was not precipitated when Tau PFF was omitted or when a control antibody was used (lanes 7, 8). We conclude that ITGαV/β1 also interacts with Tau PFFs and thus may serve as a receptor for both monomeric and filamentous Tau.

We next tested whether ITGαV/β1 mediates Tau PFF cell entry. We generated lentiviruses expressing small hairpin RNAs (shRNAs) that specifically knocked down *ItgαV* or *Itgβ1* (Figure 2b, c). Knockdown of *ItgαV* and *Itgβ1* either individually or in combination did not affect the viability of astrocytes, but significantly reduced Tau PFF internalization (Supplementary Fig. 3b, Figure 2d, e, f). Furthermore, knockdown of *Talin1*, an adaptor essential for integrin signaling and integrin-mediated endocytosis [41-43] also led to a significant reduction in Tau PFF uptake (Figure 2e, f, g). The fact that knockdown of three

different integrin pathway components all reduced Tau PFF uptake ruled out the possibility of an off-target effect. Intriguingly, treating cells with a potent inhibitor (PF-562271) of the focal adhesion kinase (FAK), an essential integrin regulatory kinase downstream of Talin1 did not affect Tau PFF endocytosis (Figure 2h, i), nor did it affect cell viability (Supplementary Fig. 3c). These results suggest that binding to ITGαV/β1 triggers Tau PFF cell entry, which requires Talin1 but not the downstream integrin signaling.

Monomeric Tau and Tau PFFs differentially activate integrin signaling

The ligation of ligands such as fibronectin to integrin activates integrin signaling, changing the expression of many downstream genes [44]. To test whether Tau also activated integrin signaling, we treated primary astrocytes with monomeric Tau, Tau PFFs, or as a control with phosphate buffer saline (PBS) for 6 h. qRT-PCR analyses of a collection of integrin target genes (*Mmp9*, *Icam1*, *Mmp13* etc.) [45, 46] showed that compared to PBS-treated cells, Tau monomer and PFFs differentially activated the expression of many integrin target genes with Tau PFF being ~2-3fold more potent than monomeric Tau (Figure 3a). As anticipated, PFF-induced integrin activation could be mitigated if astrocytes were first infected with lentiviruses that knocked down *ItgαV* and *Itgβ1* (Figure 3b).

Because astrocytes purified by the conventional method also contain some microglia and oligodendrocytes, we used immunopanning-purified astrocytes to further validate Tau PFF-induced integrin signaling (Figure 3c) (see the methods). Immunostaining using an antibody against the astrocyte-specific marker GFAP showed

that purified astrocytes were free of other cell types. Immunopurified astrocytes internalized Tau PFFs similarly as conventionally purified astrocytes (Figure 3c). These cells also activated integrin target genes after being stimulated by Tau PFFs (Figure 3d), which was reproducibly diminished when Talin1 was depleted (Figure 3d). Altogether, these data suggest that like canonical integrin ligands, the interactions of Tau and Tau PFFs with ITGαV/β1 also activate integrin signaling.

Tau PFFs induce astrocytic inflammation via αV/β1 integrin

As a major immune-competent cell in the CNS, astrocytes can sense danger signals and elicit an immune response via the secretion of pro- or anti-inflammation cytokines and chemokines [28, 47]. We analyzed the mRNA expression of a collection of cytokine and chemokine genes by qRT-PCR in astrocytes exposed to Tau monomer or Tau PFFs using PBS-treated cells as a reference. Intriguingly, PFF treatment caused a strong induction of several pro-inflammatory cytokines (*IL1α*, *IL1β*, *IL6*, *TNFα*) and chemokines (*Ccl2*, *Ccl3*, *Ccl4*, *Cxcl10*). By contrast, the expression of *Clc12* and several anti-inflammation cytokines/chemokines such as *IL10* and *TGFβ* was not affected (Figure 4a, b). Monomeric Tau also activated pro-inflammatory cytokines/chemokines, but consistently to lower levels (Figure 4a, b), suggesting that integrin activation by Tau might be coupled to inflammation induction. Indeed, the induction of pro-inflammatory genes by Tau PFFs was largely abolished in integrin αV/β1 knockdown astrocytes (Figure 4c). Thus, ITGαV/β1 is required for a Tau PFF-induced pro-inflammation response in astrocytes.

Astrocyte activation is usually linked to increased expression of the NO synthase (*NOS2*) [48], which upregulates the production of nitric oxide (NO) during inflammation [49]. Indeed, qRT-PCR detected a significant increase in the expression of *NOS2* in astrocytes following Tau PFF treatment. Like integrin target genes, *NOS2* expression was also induced by monomeric Tau, albeit by a smaller magnitude (Figure 4d), and the depletion of *ItgαV/β1* significantly reduced Tau PFF-induced *NOS2* expression (Figure 4e).

Tau PFF-induced inflammation requires Talin1 and FAK

To further elucidate the functional link between Tau PFF-induced integrin signaling and astrocytic inflammation, we used immunopurified astrocytes to test the requirement of Talin1 and FAK in PFF-induced inflammation. As expected, Tau PFF treatment induced the expression of pro-inflammation cytokines and chemokines such as *IL1α*, *IL1β*, *IL6*, *TNFα*, *Ccl2*, *Ccl3*, *Ccl4*, *Cxcl10* as well as the *IL1* downstream gene *NOS2*, but noticeably, the induction of *IL1α*, *IL1β* and *NOS2* by Tau PFF was much higher than that seen in conventionally purified astrocytes (Figure 4f-i). This was probably due to the use of integrin antibodies during the purification (Figure 3c), which might enrich a population of astrocytes with high integrin expression. As anticipated, lentivirus-mediated knockdown of *Talin1* reproducibly reduced Tau PFF-induced expression of pro-inflammation cytokines, chemokines and *NOS2* (Figure 4f-i).

To test the role of FAK in Tau PFF-induced inflammation, we pre-treated immunopurified astrocytes with the FAK inhibitor PF-562271, which dose-dependently

abolished Tau PFF-induced expression of pro-inflammatory genes (Supplementary Fig. 4a, Figure 4j, k). Thus, Tau PFF-induced inflammation requires Talin1 and FAK.

Tau PFFs activate NFκB via the integrin signaling

Because NFκB is a central regulator of inflammation and because integrin activation has been linked to NFκB signaling [50, 51], we used qRT-PCR to measure the expression of *NFκB* in PFF- and monomeric Tau-treated astrocytes. For comparison, we also tested *STAT3*, another inflammation regulatory transcription factor [52]. Indeed, *NFκB* but not *STAT3* was activated by Tau PFFs and also to a lesser extent by monomeric Tau (Figure 5a). Additionally, PFF-induced NFκB expression was mitigated either by knockdown of *ItgαV/β1* or *Talin1,* or by the FAK inhibitor PF-562271 (Figure 5b-d). Immunostaining using a NFκB specific antibody detected NFκB p65 mostly in the cytoplasm in control cells, but treatment with either monomeric Tau or Tau PFF caused an increase in the nuclear/cytoplasmic NFκB ratio (Figure 5e-g), further confirming the activation of NFκB by Tau. These findings, together with the observations that Tau-induced inflammatory gene expression was abolished by a NFκB inhibitor (Supplementary Fig. 4b, Figure 5h, i) suggest that Tau PFFs induce an inflammation response in astrocytes as a result of NFκB activation via integrin signaling.

Tau PFF converts astrocytes into a neurotoxic state via αV/β1 integrin

A recent study suggested that extracellular factors in the brain microenvironment can

cause native astrocytes to adopt different functional states [30]. These states are linked to the expression of pan-reactive genes and certain A1- or A2-specific genes. Since Tau PFFs activate integrin signaling and induce inflammation, we tested whether PFF-treated astrocytes resemble the neurotoxic A1 state or the neuroprotective A2 state by determining the expression of the previously characterized pan-reactive, A1 and A2 signature genes. Interestingly, qRT-PCR showed that both Tau monomer and PFFs induced the expression of many pan-reactive and A1 specific genes such as *Gbp2*, *H2-T23*, *Ggta*, *Ligp1*, *Psmb8* etc with PFFs generally causing a higher level of induction than monomer (Figure 6a). By contrast, most A2 genes were not significantly affected with the exception of *Cd14*, *Tgm1*, and *Ptx3*. Thus, monomeric Tau and Tau PFF appear to convert astrocytes into an A1-like state. Knockdown of either *ItgαV/β1* or *Talin1* dramatically reduced Tau PFF-associated gene induction (Figure 6b, c, Fig. S5), so did the treatment with PF-562271 and the NF κB inhibitor PDTC (Pyrrolidine dithiocarbamate) [50] (Figure 6d, e) . Thus, Tau PFFs alter astrocytes in an integrin-dependent manner, converting them to an A1-like state.

Tau PFF-treated astrocytes release neurotoxic factors

To further test whether Tau PFFs converted astrocytes into a neurotoxic state, we treated astrocytes with PBS, monomeric Tau, or Tau PFFs for 6 h and then replated these cells in a Tau-free medium for 48 h. After incubation, many cells treated by Tau PFFs displayed a tadpole-like morphology, which was not seen in monomeric Tau or PBS-treated samples

(Supplementary Fig. 6a). We then used the conditioned medium (CM) from these cells to treat mouse cortical neurons. No Tau carryover was detected in CM (Supplementary Fig. 6b). However, when neuronal cell death was monitored 72 h later by a fluorescence-based cell viability assay (Figure 7a), the CM from Tau PFF-treated cells was significantly more toxic than that from PBS- or monomeric Tau-treated astrocytes. Interestingly, the CM from PFF-treated, ITGαV/β1 knockdown astrocytes had a significantly reduced neurotoxic activity compared to the CM from PFF-treated control cells (Figure 7b, c). These results suggest that Tau PFF-treated astrocytes release a neurotoxic factor(s) in an ITGαV/β1-dependent manner.

Discussion

The accumulation and propagation of Tau filamentous aggregates are observed in a broad spectrum of neurodegenerative disorders including AD [1, 53]. The progressive spreading of Tau inclusions, which has been recapitulated in mouse models [4, 5, 54], is thought to take place along neuronal connections or via unconventional protein secretion followed by cell uptake [7, 55]. Tau-containing aggregates have also been detected in glial cells (both microglia and astrocytes), although endogenous Tau is not expressed in these cells. This suggests that pathological Tau inclusions may also be transmitted from neurons to glia [56-59]. Importantly, expression of human Tau in glia in a *Drosophila* model led to neurotoxicity, suggesting that Tau, if propagated into glial cells, might have a pathogenic activity [60]. Likewise, in a transgenic mouse model, astrocytic expression of human Tau using the

astrocyte-specific GFAP (glial fibrillary acidic protein) promoter leads to neurodegeneration [61]. These results demonstrate that the prion-like transmission of Tau aggregates from neurons to glia may contribute to neurodegeneration. However, it is unclear whether it is the internalized Tau fibrils or an interplay between the extracellular Tau and a cell surface receptor(s) that causes neurotoxicity.

In this study, we show that Tau filamentous aggregates bind to an integrin receptor complex (ITGαV/β1) on the astrocyte surface, which not only mediates Tau fibril uptake, but also regulates fibril-induced inflammation and astrocytic conversion (Figure 7d). ITGαV/β1, as a member of the integrin family, is a cell surface adhesion molecule that binds to extracellular matrix proteins [44]. This activates integrin signaling, which has been linked to cancer cell invasion and proliferation [44, 46]; Through the actin-binding protein Talin1 and the downstream focal adhesion kinase (FAK), integrin activation alters gene expression, allowing cancer cells to adapt to the constantly changing microenvironment during metastasis. Integrins and their ligands are also widely expressed in the CNS where they support neural development [62, 63]. Moreover, several lines of evidence have hinted at a role for integrins in proteotoxic stress-associated neurodegeneration: 1) A genome-wide association study (GWAS) in a *Drosophila* model of AD identified fly homologs of the human integrin receptors ITGαM and ITGα9 as modifiers for Tau-induced neurotoxicity [36]; 2) Microglia can take up fibrillar AD-associated β-Amyloid (Aβ) aggregates via ITGα6/β1 and an integrin-associated protein CD47 [39]; 3) The expression of β1 integrin is elevated in cortical astrocytes from AD patients, and in AD-related animal models β1 integrin can

mediate soluble Aβ oligomers-induced astrogliosis [64]; 4) A more recent study revealed that in response to spinal cord injury, which is often associated with the release of stress-inducing factors such as misfolded proteins, astrocytes are activated via an integrin and cadherin-dependent mechanism to form astrocytic scars [65]. In light of these observations and our findings, we propose that integrin receptors on astrocytes may sense extracellular misfolded proteins, initially facilitating their clearance, but eliciting a danger signaling in the form of inflammation when overburdened by misfolded proteins. This model does not exclude the possibility that the astrocytic inflammation status may be partially modulated by endocytosed Tau-integrin complex or by a combined activation of integrin and other cell signaling pathways on the cell surface.

Intriguingly, Tau fibrils and monomers can differentially activate integrin signaling, which might be due to their different oligomeric states. In support of this view, recent studies have underscored the role of liquid-liquid phase separation in transmembrane receptor signaling [66]. Specifically, the coagulation of membrane receptors into a gel-like state upon binding to a multivalent ligand can dramatically amplify the magnitude of downstream signaling. Indeed, receptor clustering upon binding of a multivalent ligand is known to potentiate the outside-in integrin signaling [67].

Astrocytes, as the most abundant glial cells in the CNS, are a well-established modulator of neurodegeneration-associated inflammation [47]. Specifically, disease-associated abnormal proteins such as Aβ and α-Syn fibrils can change astrocyte physiology. For instance, different Aβ species can activate disparate astrocytic cell

receptors to induce the pro-inflammatory NF-κB pathway [68-71]. Our study shows that extracellular Tau aggregates can impact astrocytes similarly, suggesting a unified interplay between extracellular misfolded proteins and astrocytes.

Importantly, our study shows that Tau PFF-activated astrocytes resemble the neurotoxic A1 state reported recently [30]. This gain-of-function state, which has been associated with astrocytic inflammation, was suggested to play a causal role in neurodegeneration, but the upstream signals that promote astrocytic activation are unclear. Particularly, existing evidence suggests that the A1 state could only be achieved by a relayed signal elicited from microglial cells exposed to an extracellular insult such as LPS. By contrast, we showed that even in the absence of microglia, misfolded Tau aggregates can trigger astrocyte activation via ITGαV/β1. This suggests that astrocytic inflammation may be a key contributor to tauopathies. Additionally, given that neurons are usually the major source of secreted Tau, our findings raise the possibility that astrocytes may monitor the healthy state of neurons by sensing the level of misfolded Tau released. It is conceivable that Tauopathies in neurons at low levels may be mitigated by intercellular transmission and astrocyte-mediated clearance, but at high levels will activate astrocytes, which release neurotoxic factors to cause neurodegeneration. This model opens a venue for drug development aimed at preventing astrocytic activation in tauopathies.

Methods

Animals and reagents

Wild-type C57BL/6J mice were purchased from the Jackson Laboratories. All animals were maintained in accordance with the animal care standards of the National Institutes of Health. All reagents are listed in Supplementary table 1.

Conventional primary astrocyte culture

Primary astrocyte cultures were prepared from cerebral cortices of P2-P5 C57BL/6J mice. Cortices were dissected, stripped of meninges, and digested with 0.25% trypsin at 37 °C in Hank's Balanced Salt Solution (HBSS) (Thermo Fisher) for 10 min. Trypsinization was stopped by the addition of astrocyte culture medium (DMEM/ F12 50/50 (Thermo Fisher) containing 25 mM glucose, 4 mM glutamine, 1 mM sodium pyruvate, and 10% FBS). Single-cell suspension of the digested tissue was obtained by repeated pipetting. Cells were seeded into a 75 ml flask at a density of ~4×10^5 cells/cm^2 and cultured in astrocyte culture medium at 37 °C in a humidified 5% CO_2 incubator. Monolayers of glial cells were obtained 7-10 days after plating. To remove microglia, cultures were gently shaken, and the floating cells (microglia) were removed, resulting in more than 95% pure astrocytes. The remaining astrocytes were incubated for 72 h before being infected with lentivirus or other experiments. Before experiments, astrocytes were dissociated by trypsinization and then reseeded at 4×10^5 cells cm^2 or 1.5×10^5 cells per well in 24-well or 1.5×10^6 cells per well in 6-well or 2×10^5 cells cm^2 in Labtek imaging dish in DMEM F12 50/50 containing 10% FBS and 1% penicillin-streptomycin. At the start of each experiment, the medium was

changed to regular DMEM without serum and antibiotics.

Primary astrocyte culture purified by immuno-panning

Astrocytes were purified by immune-panning from P2-P5 C57BL/6J mice and cultured as previously described [72]. Briefly, cortices were digested by Trypsin at 37 °C and then mechanically dissociated to generate single-cell suspension, which was incubated in successive negative immune-panning plates to remove macrophage and microglia cells before positive selection for astrocytes by an ITGβ5-coated panning plate. Isolated astrocytes were cultured in a defined, serum-free base medium containing 50% neurobasal, 50% DMEM, 100 U/ml penicillin, 100 μg/ml streptomycin, 1 mM sodium pyruvate, 292 μg/ml L-glutamine, 1 x G5 supplement. This medium was supplemented with the astrocyte-required survival factor HBEGF (Peprotech, 100-47) at 5 ng/ml as previously described [73].

Primary neuron cultures

Primary neuron cultures were either purchased from Thermo Fisher Scientific or prepared from cerebral cortices of P0-P1 C57BL/6 mice. Cortices were dissected, stripped of meninges, and digested with 0.25% trypsin at 37 °C in HBSS for 10 min. Trypsinization was stopped by the addition of FBS. A single-cell suspension of the digested tissue was obtained by repeated pipetting. Cells were seeded into a 24 well plate at a density of 1.5 x 10^5 cells per well and cultured in DMEM culture medium supplemented with 10% fetal bovine serum (Thermo Fisher), 100 U/ml of penicillin, 0.1 mg/ml of streptomycin (Thermo Fisher), 25 mM glucose, 4 mM glutamine, and 1 mM sodium pyruvate at 37 °C. At 24 h

after seeding, the medium was changed with Neurobasal medium (Thermo Fisher) supplemented with B-27 (Thermo Fisher) containing 0.5 mM glutamine. Cells were cultured at 37 °C in a humidified chamber supplemented with 5% CO2. Cultures were used for experiments from 7 to 10 days after seeding.

Purification of Tau protein

The recombinant human (Tau 2N4R isoform), containing 2 N-terminal inserts and 4 microtubule binding repeats was isolated as previously described [31]. Briefly, the untagged Tau protein was expressed using the pET29b vector in the *E.coli* strain *BL21*. From a culture volume of 10 liter, the cell pellet was resuspended in ice cold cell resuspension buffer (20 mM MES, 1 mM EGTA, 0.2 mM $MgCl_2$, 5 mM DTT, 1 mM PMSF). Cells were disrupted by sonication, and NaCl was added to a final concentration of 500 mM. Cell suspension was boiled for 20 min, which denatured almost all proteins except for Tau. The denatured proteins and insoluble cell debris were sedimented by centrifugation at 127,000g for 40 min at 4 °C. The supernatant was dialyzed overnight twice in the cation exchange chromatography buffer A (20 mM MES, 50 mM NaCl, 1 mM EGTA, 1 mM $MgCl_2$ with 2 mM DTT, 0.1 mM PMSF at 4 degree under constant stirring. Cleared the dialysate by centrifugation at 127,000g for 40 min at 4 °C. The clear supernatant was loaded onto a cation-exchange chromatography column. The bound Tau protein was eluted with a linear gradient of 0-60% final concentration of the cation exchange chromatography buffer B (20 mM MES, 1 M NaCl, 1 mM EGTA, 1 mM $MgCl_2$, 2 mM DTT, 0.1 mM PMSF) over 6 column volumes. Fractions containing Tau were pooled and concentrated by an

ultrafiltration device (Millipore 10 kDa MW cutoff) to a final volume of 1 ml. Concentrated Tau protein was further fractionated by a size exclusion column in a gel filtration buffer (PBS with 1mM DTT), flash-frozen in liquid nitrogen and stored at -80 °C. 50 μM purified Tau was labeled with Alexa Fluor 594 dye following the manufacturer's instruction (Thermo Fisher).

Preparation of paired helical filaments from Tau proteins

The condition for Tau polymerization is: 50 μM purified Tau protein, 12.5 μM heparin, a protease inhibitor cocktail (10 μg/ml leupeptin, 5 μg/ml chymostatin, 3 μg/ml elastatinal, and 1 μg/ml pepstatin), and 2 mM DTT in phosphate buffer saline (PBS). This solution was incubated at 37 °C for two weeks. Tau polymerization is induced by the addition of heparin. 1mM fresh DTT was added into the solution every 24 h to maintain reducing condition since disulfide bond formation in the four-repeat domain of Tau reduces polymerization efficiency. After polymerization, Tau filaments were dialyzed extensively with PBS to remove heparin and DTT. Transmission electron microscopy was used to check PHF assembly.

Electron microscopy (EM) analysis of Tau filaments

5 mg/ml Tau filaments were diluted 10-fold in PBS and loaded onto an EM grid. The grid was then washed with pure water and stained with 3% uranyl acetate for 1 min and then imaged with a Morgagni 268 transmission electron microscope.

Tau internalization assay

Tau fibrils were diluted in PBS and sonicated with 10 pulses of 30 % amplitude before being added to culture medium. Primary astrocyte culture was treated with 200 nM Tau filament-Alexa Fluor 594 for 2 hours in the astrocyte culture medium. In the case of inhibitor treatment, culture was pretreated with 10 μM PF262271 for 2 hours. Cells were either directly imaged using a Zeiss LSM780 confocal microscope or fixed with 4% paraformaldehyde in PBS before imaging.

RNA isolation and gene expression analysis.

RNA isolation was performed using a RNeasy Mini Kit (Qiagen) according to the manufacturer's protocol. RNA concentration was measured using Nanodrop-1000. Complementary DNA synthesis was performed using an iScript™ Reverse Transcription Supermix for RT-qPCR (Bio-Rad) according to the manufacturer's instructions, with a minimal input of 200 ng total RNA. Quantitative PCR (qPCR) was performed using a CFX96 Touch Real-Time PCR Detection System (Bio-Rad) using cDNA amount equivalent to 1–2 ng total RNA during cDNA synthesis. SsoAdvanced Universal SYBR Green Supermix (Bio-Rad) and a 2 pmol/ml mixture of forward and reverse primers were used for 45 cycles of gene amplification. The primers used for qPCR are listed in Supplementary Table 2. GAPDH mRNA was used as an internal reference. The CFX manager software was used to analyze the qPCR results. To calculate fold changes, we used PBS-treated samples as a reference.

Lentivirus production and infection

For Lentivirus production, two 15 cm dishes of HEK293FT cells were seeded at 40%

confluence. On the next day, 1 h prior to transfection, the medium was replaced with 13 ml pre-warmed Opti-MEM medium (Thermo Fisher). Transfection was performed using Lipofectamine 2000 and the PLUS reagent (Thermo Fisher). For each dish, 6.8 μg pCMV-VSV-G, 10.1 μg psPAX2 (Addgene), 13 μg gene-specific lentiviral shRNA plasmids and 135 μl of PLUS reagent (Thermo Fisher) were added to 4 ml Opti-MEM as mixture A, which is then mixed with mixture B containing 68 μL lipofectamine 2000 and 4 ml Opti-MEM. The complete mixture was incubated for 20 min at room temperature and then added to cells. After 6 h, the medium was changed to 25 ml D10 medium (DMEM medium with 10% FBS and 1% Bovine Serum Albumin) with antibiotics (penicillin/streptomycin, 10 U/ml) for virus production. After 60 h of incubation, virus-containing medium from two culture dishes were combined and centrifuged at 2,000 g at 4 °C for 10 min to pellet cell debris. The supernatant was filtered through a 0.45 μm low protein-binding membrane (Steriflip HV/PVDF, Millipore). To concentrate lentivirus, the cleared supernatant was ultracentrifuged at 47,000 g for 2 hours at 4 °C using the JA25.50 rotor (Beckman). The virus was resuspended overnight in 180 μL D10 medium at 4 °C. Virus was aliquoted, flash-frozen in liquid nitrogen and stored at −80 °C. For infection, 10 μl concentrated virus was directly added to astrocytes cultured in 6 well. The medium was changed 24 hours after infection, and the knockdown efficiency was evaluated by qRT-PCR 96 h post-infection.

Cell lines and DNA transfection

HEK293T and SH-SY5Y cells were purchased from ATCC. HEK293FT cells were from

Thermo Fisher. HEK293T and HEK293FT Cells were maintained in Dulbecco's Modified Eagle's Medium (DMEM, Corning) containing 10% fetal bovine serum (FBS) and antibiotics (penicillin/streptomycin, 10 U/ml). SH-SY5Y cells were maintained in DMEM/ F12 50/50 (Thermo Fisher) containing 10% fetal bovine serum (FBS) and antibiotics (penicillin/streptomycin, 10 U/ml). All cell lines were maintained at 37 °C. Cell transfections were performed using TransIT-293 reagent (Mirus) for HEK293T or Lipofectamine 2000 (Thermo Fisher) for SH-SY5Y cells following the manufacturer's instructions.

Immunoblotting

Immunoblotting was performed using a standard protocol. Proteins were separated in NuPAGE (4%–12%) Bis-Tris gels (Thermo Fisher) and transferred onto nitrocellulose membranes (Bio-Rad). The target protein was detected by specific primary antibodies followed by secondary horseradish peroxidase (HRP)-conjugated antibodies (for less abundant proteins) (Sigma) or fluorescence-labeled secondary antibodies (for abundant antigens) (Thermo Fisher). For immunoblotting with HRP-conjugated secondary antibodies, the signal was detected by the enhanced chemiluminescence method (ECL) using the Immobilon western chemiluminescent HRP substrate (Millipore) and recorded by a Fuji LAS-4000 image reader. The intensity of the detected protein bands was quantified by ImageGauge v3.0 software. For immunoblotting with fluorescence-labeled secondary antibodies, membranes were scanned using a LI-COR Odyssey scanner. The intensity of the protein bands was quantified by the LI-COR Odyssey v3.1 software.

Cell surface binding assay and biotinylated samples preparation for MS proteomics

Cells were washed with pre-cold PBS two times to remove serum completely. We prepared 200 nM Tau-Apex2 or Apex2 proteins in serum-free pre-cold F-12 medium (5 ml for each 15 cm petri dish). We incubated cells with these proteins for 30 minutes at 4℃ with gentle shaking. After incubation, we removed the unbounded proteins by thoroughly washing the cells 3 times, each with 6 ml pre-cold F12 medium. We then incubated cells in 500 μM Biotin-phenol (BP) in F-12 serum-free medium (10 ml for one 15 cm petri-dish) pre-warmed to 37 ℃. After 30 minutes of incubation, we added freshly prepared H_2O_2 stock solution (100 mM) into the cells to achieve a final concentration of 1 mM. Cells were incubated further at room temperature for 4 min. The medium was removed and cells were washed twice with the quencher solution (10 mM sodium ascorbate, 5 mM Trolox, and 10 mM sodium azide in DPBS.), followed by two washes with DPBS, and then resuspended in the quencher solution. Collect Cells were pelleted by centrifugation at 3,000 g for 10 min at 4℃, lysed in 7 ml PBS-based lysis buffer with 0.5% NP40, a protease inhibitor cocktail, 1 mM DTT, 10 mM sodium azide, 10 mM sodium ascorbate and 5 mM Trolox). After incubation on ice for 40 min, cell extracts were cleared by centrifugation at 15,000 g for 10 min at 4 ℃. Cleared supernatant was incubated with 50 μl pre-washed streptavidin beads, gently rocked at 4 ℃ for 1 h. The beads were extensively washed with PBS containing 0.05% NP40. Bound proteins were eluted in 50 μl 1x sample buffer. Proteins

were fractionated on a SDS-PAGE gel. Proteins in excised bands were identified by the Taplin Mass Spectrometry core at Harvard Medical School as fee for service.

Survival/cell toxicity assay.

Astrocytes were infected with shRNA-expressing lentivirus on 72 h after plating. Cells were grown for a total of 7 days in serum-free medium supplemented with 5 ng/ml HBEGF18 in 6 well plate. Cells were then treated with 200 nM Tau PFFs or an equivalent volume of DPBS (as a control) for 6 h, then washed extensively to remove remaining Tau filaments. To further ensure that no Tau filaments were carried over to conditioned medium, cells were trypsinized and then re-seeded into a new 6 well plate, grown for an additional 48 h. At this time, the conditioned medium was collected and a protease inhibitor cocktail was added to inhibit protein degradation. Conditioned medium was concentrated ~40 times by Amicon Ultra-15 Centrifugal Filter Units with 30 kDa cutoff filter (Millipore, UFC903024), and then added to primary neuron cultures at 10 days in vitro (plated at 1.5 × 10^5 cells per well in a poly-D-lysine-coated 24-well plate). The viability assay was performed 72 h later using the Live/Dead Kit (Thermo Fisher Scientific, L3224).

Image acquisition and processing,

Confocal microscopy was performed on a Zeiss LSM780 laser scanning confocal microscope (63X/1.46 objective) with the Zen program. Image processing was done using the open source ImageJ (Fiji) software. Images were converted to individual channels and regions of interest were drawn for intensity measurement. For dead cell counting, single channel images were converted to black and white. A constant threshold was applied to

all the images for dot counting.

Statistics and reproducibility

Statistical analyses were performed using either Excel or Prism 8. Data are presented as mean ± SEM, calculated by GraphPad Prism 8, and *p*-values were calculated by student's t-test using Excel. The n values in the figure legends indicate independent experimental repeats. Images were prepared with Adobe Photoshop and graphs were plotted by GraphPad Prism 8.

Figure 1c is a representative gel from two independent biotin pulldown experiments. Figure 1d-f, Figure 2a, Supplementary Figure 2a, b, e; 3a show representative gels from three independent experiments. Supplementary Figure 1c, 2c, 3b, c; 6a, b show negative controls that were only performed once.

Data availability

All data generated for this study are included in this article and its supplementary materials. Source data is available from the corresponding author upon reasonable request.

References

1. Lee, V.M., Goedert, M. & Trojanowski, J.Q. Neurodegenerative tauopathies. *Annu Rev Neurosci* **24**, 1121-1159 (2001).
2. Spillantini, M.G. & Goedert, M. Tau pathology and neurodegeneration. *Lancet Neurol* **12**, 609-622 (2013).
3. Frost, B. & Diamond, M.I. Prion-like mechanisms in neurodegenerative diseases. *Nat Rev Neurosci* **11**, 155-159 (2010).
4. Clavaguera, F. *et al.* Transmission and spreading of tauopathy in transgenic mouse brain. *Nat Cell Biol* **11**, 909-913 (2009).
5. Stancu, I.C. *et al.* Templated misfolding of Tau by prion-like seeding along neuronal connections impairs neuronal network function and associated behavioral outcomes in Tau transgenic mice. *Acta Neuropathol* **129**, 875-894 (2015).
6. Mudher, A. *et al.* What is the evidence that tau pathology spreads through prion-like propagation? *Acta Neuropathol Commun* **5**, 99 (2017).
7. Ye, Y. Regulation of protein homeostasis by unconventional protein secretion in mammalian cells. *Semin Cell Dev Biol* **83**, 29-35 (2018).
8. Saman, S. *et al.* Exosome-associated tau is secreted in tauopathy models and is selectively phosphorylated in cerebrospinal fluid in early Alzheimer disease. *J Biol Chem* **287**, 3842-3849 (2012).
9. Pooler, A.M., Phillips, E.C., Lau, D.H., Noble, W. & Hanger, D.P. Physiological release of endogenous tau is stimulated by neuronal activity. *EMBO Rep* **14**, 389-394 (2013).
10. Wu, J.W. *et al.* Small misfolded Tau species are internalized via bulk endocytosis and anterogradely and retrogradely transported in neurons. *J Biol Chem* **288**, 1856-1870 (2013).
11. Chai, X., Dage, J.L. & Citron, M. Constitutive secretion of tau protein by an unconventional mechanism. *Neurobiol Dis* **48**, 356-366 (2012).
12. Santa-Maria, I. *et al.* Paired helical filaments from Alzheimer disease brain induce intracellular accumulation of Tau protein in aggresomes. *J Biol Chem* **287**, 20522-20533 (2012).
13. Fontaine, S.N. *et al.* DnaJ/Hsc70 chaperone complexes control the extracellular release of neurodegenerative-associated proteins. *EMBO J* **35**, 1537-1549 (2016).
14. Xu, Y. *et al.* DNAJC5 facilitates USP19-dependent unconventional secretion of misfolded cytosolic proteins. *Cell Discov* **4**, 11 (2018).
15. Martini-Stoica, H. *et al.* TFEB enhances astroglial uptake of extracellular tau species and reduces tau spreading. *J Exp Med* **215**, 2355-2377 (2018).
16. Frost, B., Jacks, R.L. & Diamond, M.I. Propagation of tau misfolding from the outside to the inside of a cell. *J Biol Chem* **284**, 12845-12852 (2009).
17. Iba, M. *et al.* Synthetic tau fibrils mediate transmission of neurofibrillary tangles in a transgenic mouse model of Alzheimer's-like tauopathy. *J Neurosci* **33**, 1024-1037 (2013).
18. Evans, L.D. *et al.* Extracellular Monomeric and Aggregated Tau Efficiently Enter Human Neurons through Overlapping but Distinct Pathways. *Cell Rep* **22**, 3612-3624 (2018).
19. Holmes, B.B. *et al.* Heparan sulfate proteoglycans mediate internalization and propagation

of specific proteopathic seeds. *Proc Natl Acad Sci U S A* **110**, E3138-3147 (2013).
20. Stopschinski, B.E. *et al.* Specific glycosaminoglycan chain length and sulfation patterns are required for cell uptake of tau versus alpha-synuclein and beta-amyloid aggregates. *J Biol Chem* **293**, 10826-10840 (2018).
21. Rauch, J.N. *et al.* Tau Internalization is Regulated by 6-O Sulfation on Heparan Sulfate Proteoglycans (HSPGs). *Sci Rep* **8**, 6382 (2018).
22. Rauch, J.N. *et al.* LRP1 is a master regulator of tau uptake and spread. *Nature* (2020).
23. Morozova, V. *et al.* Normal and Pathological Tau Uptake Mediated by M1/M3 Muscarinic Receptors Promotes Opposite Neuronal Changes. *Front Cell Neurosci* **13**, 403 (2019).
24. Allen, N.J. & Lyons, D.A. Glia as architects of central nervous system formation and function. *Science* **362**, 181-185 (2018).
25. Garcia-Caceres, C. *et al.* Role of astrocytes, microglia, and tanycytes in brain control of systemic metabolism. *Nat Neurosci* **22**, 7-14 (2019).
26. Wyss-Coray, T. *et al.* Adult mouse astrocytes degrade amyloid-beta in vitro and in situ. *Nat Med* **9**, 453-457 (2003).
27. Xiao, Q. *et al.* Enhancing astrocytic lysosome biogenesis facilitates Abeta clearance and attenuates amyloid plaque pathogenesis. *J Neurosci* **34**, 9607-9620 (2014).
28. Sofroniew, M.V. Astrocyte barriers to neurotoxic inflammation. *Nat Rev Neurosci* **16**, 249-263 (2015).
29. Ransohoff, R.M. How neuroinflammation contributes to neurodegeneration. *Science* **353**, 777-783 (2016).
30. Liddelow, S.A. *et al.* Neurotoxic reactive astrocytes are induced by activated microglia. *Nature* **541**, 481-487 (2017).
31. Barghorn, S., Biernat, J. & Mandelkow, E. Purification of recombinant tau protein and preparation of Alzheimer-paired helical filaments in vitro. *Methods Mol Biol* **299**, 35-51 (2005).
32. Perea, J.R. *et al.* Extracellular Monomeric Tau Is Internalized by Astrocytes. *Front Neurosci* **13**, 442 (2019).
33. Hung, V. *et al.* Spatially resolved proteomic mapping in living cells with the engineered peroxidase APEX2. *Nat Protoc* **11**, 456-475 (2016).
34. Brandt, R., Leger, J. & Lee, G. Interaction of tau with the neural plasma membrane mediated by tau's amino-terminal projection domain. *J Cell Biol* **131**, 1327-1340 (1995).
35. Pooler, A.M. *et al.* Dynamic association of tau with neuronal membranes is regulated by phosphorylation. *Neurobiol Aging* **33**, 431 e427-438 (2012).
36. Shulman, J.M. *et al.* Functional screening in Drosophila identifies Alzheimer's disease susceptibility genes and implicates Tau-mediated mechanisms. *Hum Mol Genet* **23**, 870-877 (2014).
37. Ajami, B. *et al.* Single-cell mass cytometry reveals distinct populations of brain myeloid cells in mouse neuroinflammation and neurodegeneration models. *Nat Neurosci* **21**, 541-551 (2018).
38. Rapisarda, V. *et al.* Integrin Beta 3 Regulates Cellular Senescence by Activating the TGF-

beta Pathway. *Cell Rep* **18**, 2480-2493 (2017).
39. Koenigsknecht, J. & Landreth, G. Microglial phagocytosis of fibrillar beta-amyloid through a beta1 integrin-dependent mechanism. *J Neurosci* **24**, 9838-9846 (2004).
40. Matter, M.L., Zhang, Z., Nordstedt, C. & Ruoslahti, E. The alpha5beta1 integrin mediates elimination of amyloid-beta peptide and protects against apoptosis. *J Cell Biol* **141**, 1019-1030 (1998).
41. Tadokoro, S. *et al.* Talin binding to integrin beta tails: a final common step in integrin activation. *Science* **302**, 103-106 (2003).
42. Sun, Z., Costell, M. & Fassler, R. Integrin activation by talin, kindlin and mechanical forces. *Nat Cell Biol* **21**, 25-31 (2019).
43. Klapholz, B. & Brown, N.H. Talin - the master of integrin adhesions. *J Cell Sci* **130**, 2435-2446 (2017).
44. Kadry, Y.A. & Calderwood, D.A. Chapter 22: Structural and signaling functions of integrins. *Biochim Biophys Acta Biomembr* **1862**, 183206 (2020).
45. Kim, C. *et al.* Neuron-released oligomeric alpha-synuclein is an endogenous agonist of TLR2 for paracrine activation of microglia. *Nat Commun* **4**, 1562 (2013).
46. Hamidi, H. & Ivaska, J. Every step of the way: integrins in cancer progression and metastasis. *Nat Rev Cancer* **18**, 533-548 (2018).
47. Colombo, E. & Farina, C. Astrocytes: Key Regulators of Neuroinflammation. *Trends Immunol* **37**, 608-620 (2016).
48. Liu, B. & Neufeld, A.H. Expression of nitric oxide synthase-2 (NOS-2) in reactive astrocytes of the human glaucomatous optic nerve head. *Glia* **30**, 178-186 (2000).
49. Bal-Price, A. & Brown, G.C. Inflammatory neurodegeneration mediated by nitric oxide from activated glia-inhibiting neuronal respiration, causing glutamate release and excitotoxicity. *J Neurosci* **21**, 6480-6491 (2001).
50. Klein, S. *et al.* Alpha 5 beta 1 integrin activates an NF-kappa B-dependent program of gene expression important for angiogenesis and inflammation. *Mol Cell Biol* **22**, 5912-5922 (2002).
51. Kaltschmidt, B. & Kaltschmidt, C. NF-kappaB in the nervous system. *Cold Spring Harb Perspect Biol* **1**, a001271 (2009).
52. Yu, H., Pardoll, D. & Jove, R. STATs in cancer inflammation and immunity: a leading role for STAT3. *Nat Rev Cancer* **9**, 798-809 (2009).
53. Braak, H. & Braak, E. Neuropathological stageing of Alzheimer-related changes. *Acta Neuropathol* **82**, 239-259 (1991).
54. de Calignon, A. *et al.* Propagation of tau pathology in a model of early Alzheimer's disease. *Neuron* **73**, 685-697 (2012).
55. Iba, M. *et al.* Tau pathology spread in PS19 tau transgenic mice following locus coeruleus (LC) injections of synthetic tau fibrils is determined by the LC's afferent and efferent connections. *Acta Neuropathol* **130**, 349-362 (2015).
56. Kahlson, M.A. & Colodner, K.J. Glial Tau Pathology in Tauopathies: Functional Consequences. *J Exp Neurosci* **9**, 43-50 (2015).

57. Bolos, M. *et al.* Direct Evidence of Internalization of Tau by Microglia In Vitro and In Vivo. *J Alzheimers Dis* **50**, 77-87 (2016).
58. Togo, T. & Dickson, D.W. Tau accumulation in astrocytes in progressive supranuclear palsy is a degenerative rather than a reactive process. *Acta Neuropathol* **104**, 398-402 (2002).
59. Ikeda, K. *et al.* Thorn-shaped astrocytes: possibly secondarily induced tau-positive glial fibrillary tangles. *Acta Neuropathol* **90**, 620-625 (1995).
60. Colodner, K.J. & Feany, M.B. Glial fibrillary tangles and JAK/STAT-mediated glial and neuronal cell death in a Drosophila model of glial tauopathy. *J Neurosci* **30**, 16102-16113 (2010).
61. Forman, M.S. *et al.* Transgenic mouse model of tau pathology in astrocytes leading to nervous system degeneration. *J Neurosci* **25**, 3539-3550 (2005).
62. Reichardt, L.F. & Tomaselli, K.J. Extracellular matrix molecules and their receptors: functions in neural development. *Annu Rev Neurosci* **14**, 531-570 (1991).
63. Clegg, D.O., Wingerd, K.L., Hikita, S.T. & Tolhurst, E.C. Integrins in the development, function and dysfunction of the nervous system. *Front Biosci* **8**, d723-750 (2003).
64. Wyssenbach, A. *et al.* Amyloid beta-induced astrogliosis is mediated by beta1-integrin via NADPH oxidase 2 in Alzheimer's disease. *Aging Cell* **15**, 1140-1152 (2016).
65. Hara, M. *et al.* Interaction of reactive astrocytes with type I collagen induces astrocytic scar formation through the integrin-N-cadherin pathway after spinal cord injury. *Nat Med* **23**, 818-828 (2017).
66. Case, L.B., Ditlev, J.A. & Rosen, M.K. Regulation of Transmembrane Signaling by Phase Separation. *Annu Rev Biophys* **48**, 465-494 (2019).
67. Shattil, S.J., Kim, C. & Ginsberg, M.H. The final steps of integrin activation: the end game. *Nat Rev Mol Cell Biol* **11**, 288-300 (2010).
68. Gonzalez-Reyes, R.E., Nava-Mesa, M.O., Vargas-Sanchez, K., Ariza-Salamanca, D. & Mora-Munoz, L. Involvement of Astrocytes in Alzheimer's Disease from a Neuroinflammatory and Oxidative Stress Perspective. *Front Mol Neurosci* **10**, 427 (2017).
69. Gonzalez-Reyes, R.E. & Rubiano, M.G. Astrocyte s RAGE: More Than Just a Question of Mood. *Cent Nerv Syst Agents Med Chem* **18**, 39-48 (2018).
70. Garwood, C.J., Pooler, A.M., Atherton, J., Hanger, D.P. & Noble, W. Astrocytes are important mediators of Abeta-induced neurotoxicity and tau phosphorylation in primary culture. *Cell Death Dis* **2**, e167 (2011).
71. Akama, K.T. & Van Eldik, L.J. Beta-amyloid stimulation of inducible nitric-oxide synthase in astrocytes is interleukin-1beta- and tumor necrosis factor-alpha (TNFalpha)-dependent, and involves a TNFalpha receptor-associated factor- and NFkappaB-inducing kinase-dependent signaling mechanism. *J Biol Chem* **275**, 7918-7924 (2000).
72. Foo, L.C. Purification of rat and mouse astrocytes by immunopanning. *Cold Spring Harb Protoc* **2013**, 421-432 (2013).
73. Foo, L.C. *et al.* Development of a method for the purification and culture of rodent astrocytes. *Neuron* **71**, 799-811 (2011).

Acknowledgements

We thank R. Tycko (NIDDK) for assistance with the negative stain EM, J. Reece (NIDDK) for imaging assistance, Q. Zhang and Y. Xu (NIDDK) for critical reading of the manuscript. P. Wang, and Y. Ye are supported by an intramural research program of NIDDK.

Author contributions

P. Wang, and Y. Ye designed the research, analyzed the data. P. Wang performed the experiments. P. Wang and Y. Ye wrote the paper together.

Competing interests

The authors declare no competing financial interest.

Figure legends

Figure 1. Identification of integrin αV/β1 as a Tau interactor in primary astrocytes.

(**a**) Schematic overview of the proximity-based proteomic mapping strategy. Tau-APEX2 (200 nM) is bound to the cell surface. Biotinylation was initiated by incubating cells with biotin-phenol (BP) in the presence of H_2O_2 for 4 mins. Biotinylated proteins were then purified by affinity chromatography using streptavidin resin.

(**b**) Coomassie blue staining of purified Tau proteins.

(**c**) Coomassie blue staining (left) and immunoblotting (IB) (right) of biotinylated proteins from primary astrocytes incubated with APEX2 or Tau-APEX2. The arrow indicates a 120kDa protein detected in Tau-APEX2-treated cells.

(**d**, **e**) Validation of Tau-APEX2-mediated biotinylation of ITGαV/β1. **d**, Tau-APEX2 was incubated with HEK293T cells transfected with either an empty vector (EV) or ITGαV-Flag. Whole cell extracts (WCE) were either directly analyzed by immunoblotting or first subjected to biotin pulldown (Bio-PD) before immunoblotting. **e**, Whole cell extracts (WCE) from primary astrocytes treated with either APEX2 or Tau-APEX2 were analyzed directly by immunoblotting or first subjected to biotin pulldown before immunoblotting.

(**f**) Co-immunoprecipitation of Tau-APEX2 with ITGαVβ1. Astrocytes were treated with Tau-APEX2 (200 nM) or PBS as a control for 30 min on ice. Cells were lysed in an NP40-containing lysis buffer. Cell lysates were subjected to immunoprecipitation with either a control IgG or a Tau specific antibody (Tau-46). Both cell lysates and precipitated proteins were analyzed by immunoblotting. Where indicated, a fraction of the remaining medium

was also analyzed by immunoblotting to show input.

Figure 2. Integrin αV/β1 and Talin1 are required for Tau PFF uptake in astrocytes.

(**a**) Co-immunoprecipitation of Tau PFF and ITGαV/β1. Astrocytes were treated with Tau PFFs or PBS as a control. Cell lysates were subjected to immunoprecipitation with either a control IgG or a Tau specific antibody (Tau-46). Both lysates and precipitated proteins were analyzed by immunoblotting. Where indicated, a fraction of the medium collected after the binding was also analyzed by immunoblotting.

(**b, c**) Quantification (mean ± SEM) of mRNA expression by qRT-PCR performed 72 h post lentiviral infection confirmed the knockdown efficiency of ITGαV (**b**), β1 (**c**). A.U. arbitrary unit. n= 3 biologically independent experiments. The numbers above indicate p values determined by two-tailed unpaired t-test.

(**d-g**) Astrocytic uptake of Tau PFFs is dependent on ITGαV/β1 and Talin1. **f**, Representative images of lentivirus-treated astrocytes incubated with Alexa594 (Red) labeled Tau-PFF (200 nM) for 2 hours. Cells were stained with Hoechst to label the nuclei (blue). Scale bar, 5 μm. **d**, **e**, Quantification of the relative Tau PFF fluorescence intensity/cell. Mean± SEM, n= 3 biologically independent experiments. The numbers and asterisks above indicate p value (****, $p<0.0001$) determined by two-tailed unpaired t-test. Dots represent the average fluorescence intensity/cell from images (>20 cells/image) acquired.

(**g**) As in **b**, except that Talin1 mRNA expression was determined after Talin1 knockdown.

Mean± SEM, n=4 biologically independent samples.

(**h**, **i**) FAK is not required for Tau PFF uptake. **h**, Representative images of DMSO or PF-562271-treated astrocytes (10 μM) incubated with labeled Tau-PFF (200 nM) after 2 hours. Scale bar, 5 μm. **i**, Quantification of Tau PFF uptake in **h**. Mean± SEM, n=3 biologically independent experiments. Dots represent average fluorescence intensity/cell from images acquired. The numbers above indicate p values determined by two-tailed unpaired t-test.

Figure 3. Monomeric and filamentous Tau differentially activate integrin signaling.

(**a, b**) Tau PFF activates integrin signaling in an ITGαV/β1 dependent manner. qRT-PCR analyses of the expression of a collection of integrin target genes in primary astrocytes. Cells were first infected with either control or ITGαV/β1 shRNA for 72 h and then treated with PBS, monomeric Tau, or Tau PFFs (200 nM) for 6 hours. Shown are fold changes (FC) normalized to PBS-treated samples. (**a**) A comparison between Tau monomer and PFF. (**b**) A comparison of Tau PFF treatment in control vs. ITGαV/β1 knockdown cells. Mean ±SEM, n=3 independent experiments, each with two technical repeats.

(**c**) A schematic overview of the immuno-panning strategy for purification of astrocytes using anti-ITGβ5 antibodies. Briefly, cortical cell suspensions were passed successively over secondary antibody-coated and anti-CD45-coated plates to remove macrophages and microglia, and then plated in a positive selection panning plate for astrocytes (anti-ITGβ5 coated). The lower panel shows a representative immunofluorescence image of purified astrocytes treated with Tau PFF Alexa594 (200 nM) (Magenta) 1h and then

stained with anti-GFAP antibodies (Green) and Hoechst (Blue). Scale bar, 5 μm.

(**d**) Talin1 is required for Tau PFF-induced integrin signaling. As in **b**, except that immunopurified astrocytes were first infected with either control- or Talin1 shRNA-expressing lentivirus and then treated with Tau PFF. Mean ±SEM n=3 independent experiments, each with two technical repeats.

The numbers and asterisks above indicate p value (****, p<0.0001) determined by two-tailed unpaired t-test.

Figure 4. Tau PFF induces inflammation in astrocytes via the integrin pathway.

(**a**-**c**) Tau PFF induces astrocytic inflammation in an ITGαV/β1 dependent manner. qRT-PCR analyses of the expression of inflammation-associated cytokine and chemokine genes in primary astrocytes. Cells were first infected with either control shRNA (**a, b**) or control and ITGαV/β1 shRNA (**c**) for 72 h and then incubated with PBS, monomeric Tau or Tau PFFs (200 nM) for 6 hours. Shown are fold changes (FC) normalized to PBS-treated cells. Mean ±SEM, n= 3 independent experiments, each with two technical repeats.

(**d**, **e**) Tau PFF induces *NOS2* expression in an ITGαV/β1 dependent manner. **d**, As in **a**, except that *NOS2* mRNA was analyzed. Mean ±SEM, n=3. Dashed lines indicate individual experiment. **e**, As in **c**, except that *NOS2* mRNA was analyzed. The number indicates p value determined by two-tailed unpaired t-test.

(**f**, **g**, **h**) qRT-PCR analyses of the expression of pro-inflammation-related cytokines (**f**, **g**) and chemokines (**h**) in immunopurified astrocytes. Cells were infected with either a control

or Talin1 (TLN1)-specific shRNA prior to the treatment with either PBS or Tau PFFs (200 nM) for 6 hours. Fold changes (FC) were normalized to PBS-treated samples. Mean ±SEM, n=6 (f, g) or n=5 (h) independent experiments, each with 2 technical duplicates.

(**i**) As in **f**, except that *NOS2* mRNA was analyzed. Mean ±SEM, n=5 independent experiments.

(**j**, **k**) qRT-PCR analyses of the expression of the indicated pro-inflammation cytokines (**j**) or chemokines (**k**) in immunopurified astrocytes that were treated with DMSO or PF-562271 (1 μM) for 1h before incubation with PBS or Tau PFF (200 nM) for 6h. Fold changes (FC) were normalized to PBS-treated samples. Mean ±SEM, n=4 (j) or 3 (k) independent experiments each with 2 technical duplicates.

The numbers and asterisks above indicate p value (****, $p<0.0001$) determined by two-tailed unpaired t-test.

Figure 5. Tau PFF-induced inflammation is dependent on NFκB activation

(**a**) qRT-PCR analyses of the expression of NFκB and STAT3 in primary astrocytes exposed to PBS, monomeric Tau or Tau PFFs (200 nM) for 6 hours. Shown are fold changes (FC) normalized to PBS-treated cells. Mean ±SEM, n=3 independent experiments each with two technical repeats.

(**b, c**) As in **a,** except that cells were first infected with control or ITGαV/β1 shRNA (**b**), or Talin1 shRNA (**c**) for 72 h and then incubated with PBS or Tau PFFs (200 nM) for 6 hours. Mean ±SEM, n=3 independent experiments.

(**d**) As in **b**, except that control- or PF-562271-treated astrocytes were used. Mean ±SEM, n=3 independent experiments.

(**e, f, g**) Tau PFF increases NFκB nuclear translocation. (**e**) Representative confocal images of astrocytes treated with either PBS, Tau monomer, PFFs (200 nM) for 4h or LPS as a positive control (5 μM) for 30min. Cell were fixed and stained with a NFκB antibody and Hoechst (blue). The graphs in **f** show the fluorescence intensity profile along the lines indicated in **e**. The blue bars indicate nuclear regions. (**g**) Quantification of the nuclear/cytoplasmic NFκB ratio in randomly selected cells. Mean ±SEM, n=3 biologically independent experiments.

(**h**, **i**) Tau PFF-induced inflammation is suppressed by a NFκB inhibitor. As in **d**, except that cells were pre-treated with PDTC (90 μM) for 1 h before Tau PFF and PBS treatment and that the indicated genes were analyzed. Mean ±SEM, n=3 independent experiments. The numbers and asterisks above indicate p value (****, $p<0.0001$) determined by two-tailed unpaired t-test.

Figure 6. Tau PFF converts astrocytes to a neurotoxic state in an integrin-dependent manner.

(**a**) A heat map shows the expression of pan-reactive, A1 and A2 signature genes in Tau monomer- and PFF-treated primary astrocytes (200 nM, 6h), which is normalized to PBS-treated cells. Shown is the average of 3 independent experiments. Asterisks indicate *p* value (*, $p<0.05$; **, $p<0.01$; ***, $p<0.001$) from two-tailed unpaired t-test.

(**b**) The expression of the indicated A1 genes were analyzed by qRT-PCR from PBS- or Tau PFF-treated (200 nM, 6h) astrocytes, which had been infected with lentiviruses (72 h) expressing control or ITGαV/β1 shRNAs. Fold changes (FC) were normalized to PBS-treated samples. Mean ±SEM, n=3 independent experiments each with 2 technical duplicates.

(**c**) As in **b**, except that immunopurified astrocytes infected with control- or Talin1 (TLN1) shRNA-expressing lentiviruses were used. Mean ±SEM, n=4 biologically independent samples.

(**d**) As in **c**, except that cells were treated with DMSO or PF-562271 (1 μM, 1h) instead of lentivirus prior to PBS or Tau PFF treatment. Mean ±SEM, n=3 biologically independent samples, each with 2 technical duplicates.

(**e**) Tau PFF-induced A1 genes is suppressed by a NFκB inhibitor. As in **d**, except that cells were treated with PDTC (90 μM) for 1 h before Tau PFF and PBS treatment. Mean ±SEM, n=3 biologically independent samples.

The numbers above indicate p value determined by two-tailed unpaired t-test.

Figure 7. Tau PFF-treated astrocytes release a neurotoxic factor(s) via ITGαV/β1 activation.

(**a**) Scheme of the cell toxicity assay.

(**b, c**) Primary cortical neurons at DIV 10 were treated with the indicated condition medium (CM) for 72 h and stained with a green-fluorescent dye calcein-AM to label viable cells

and a red-fluorescent dye ethidium homodimer-1 to label dead cells. (**b**) Representative images. Scale bar, 10 μm. (**c**) Quantification of dead cells labeled by ethidium homodimer-1 in randomly selected fields. Mean± SEM, n=3 biologically independent samples. The numbers and asterisks above indicate p value (****, $p<0.0001$) determined by two-tailed unpaired t-test.

(**d**) A working model showing the interplays between Tau-PFF, astrocytes and neurons.

Figure 1

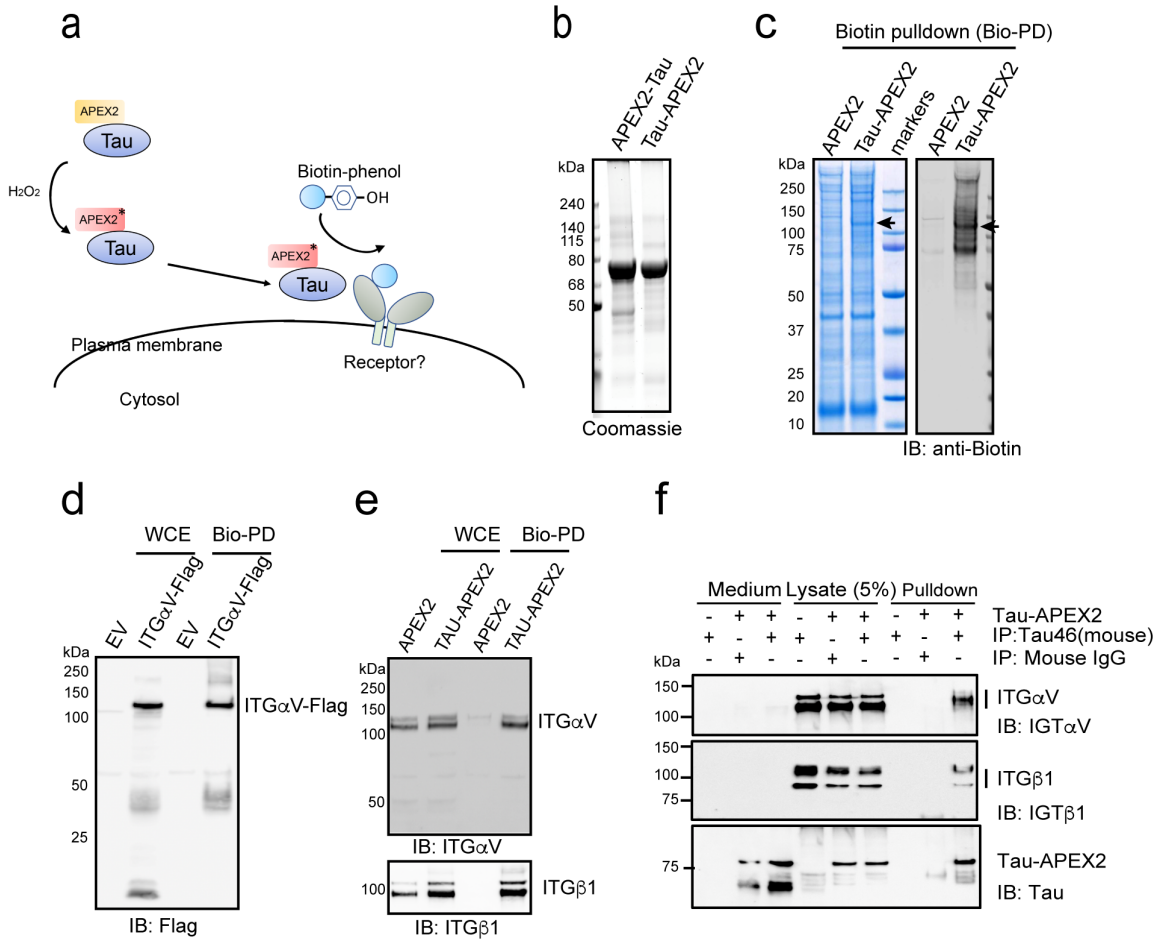
a
APEX2
Tau
H2O2
APEX2*
Tau
Biotin-phenol
OH
APEX2*
Tau
Plasma membrane
Receptor?
Cytosol
b
APEX2-Tau
Tau-APEX2
kDa
240
140
115
80
68
50
Coomassie
c
Biotin pulldown (Bio-PD)
APEX2
Tau-APEX2
markers
APEX2
Tau-APEX2
kDa
250
150
100
75
50
37
25
20
10
IB: anti-Biotin
d
WCE
Bio-PD
EV
ITGαV-Flag
EV
ITGαV-Flag
kDa
250
150
100
50
25
ITGαV-Flag
IB: Flag
e
WCE
Bio-PD
APEX2
TAU-APEX2
APEX2
TAU-APEX2
kDa
250
150
100
50
ITGαV
IB: ITGαV
100
ITGβ1
IB: ITGβ1
f
Medium Lysate (5%) Pulldown
Tau-APEX2
IP:Tau46(mouse)
IP: Mouse IgG
kDa
150
100
ITGαV
IB: IGTαV
150
100
75
ITGβ1
IB: IGTβ1
75
Tau-APEX2
IB: Tau

Figure 2

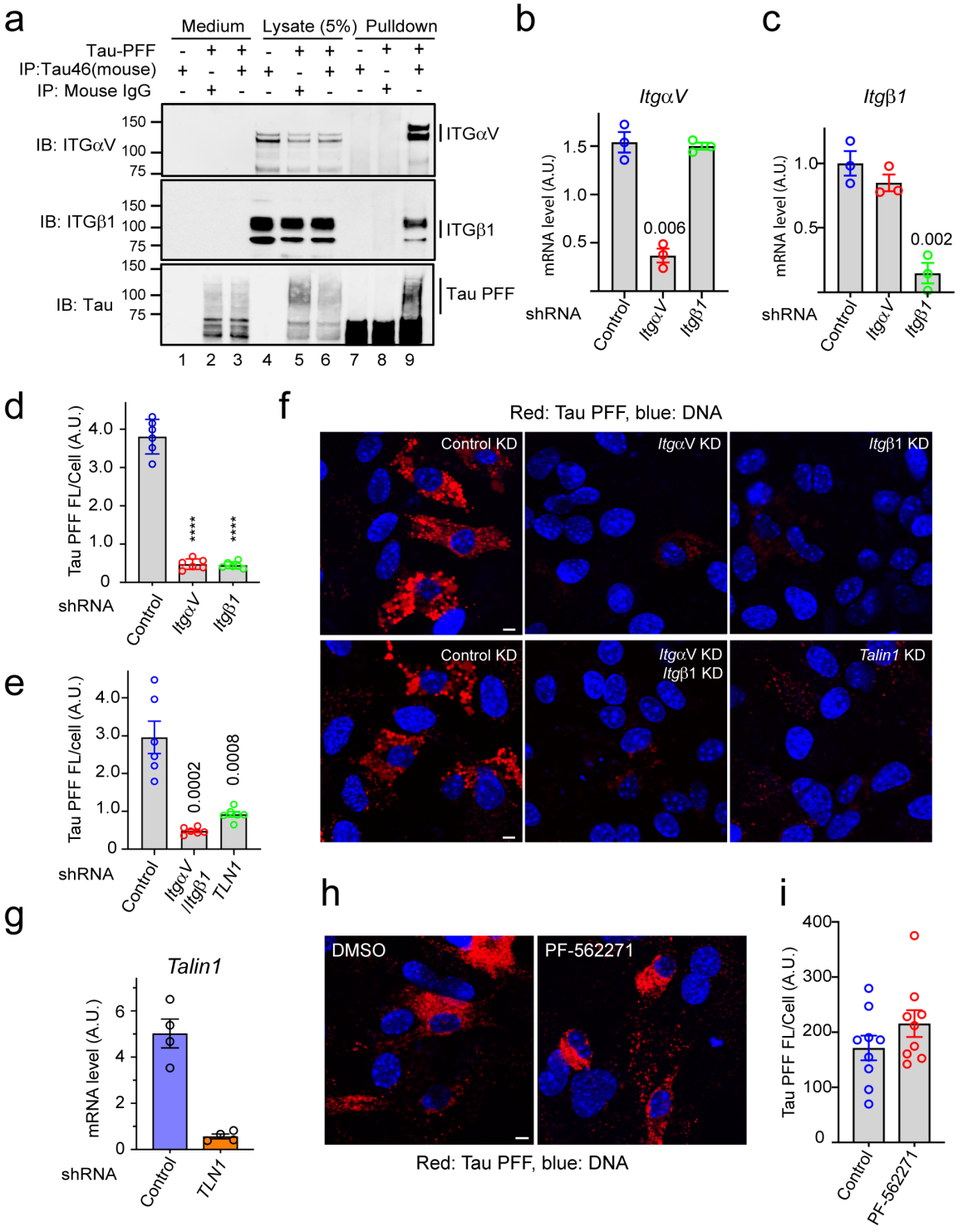
a
Medium
Lysate (5%)
Pulldown
Tau-PFF
IP:Tau46(mouse)
IP: Mouse IgG
IB: ITGαV
IB: ITGβ1
IB: Tau
ITGαV
ITGβ1
Tau PFF
b
ItgαV
mRNA level (A.U.)
0.006
shRNA
Control
ItgαV
Itgβ1
c
Itgβ1
0.002
d
Tau PFF FL/Cell (A.U.)
****
e
Tau PFF FL/cell (A.U.)
0.0002
0.0008
TLN1
f
Red: Tau PFF, blue: DNA
Control KD
ItgαV KD
Itgβ1 KD
ItgαV KD
Itgβ1 KD
Talin1 KD
g
Talin1
h
DMSO
PF-562271
Red: Tau PFF, blue: DNA
i

Figure 3

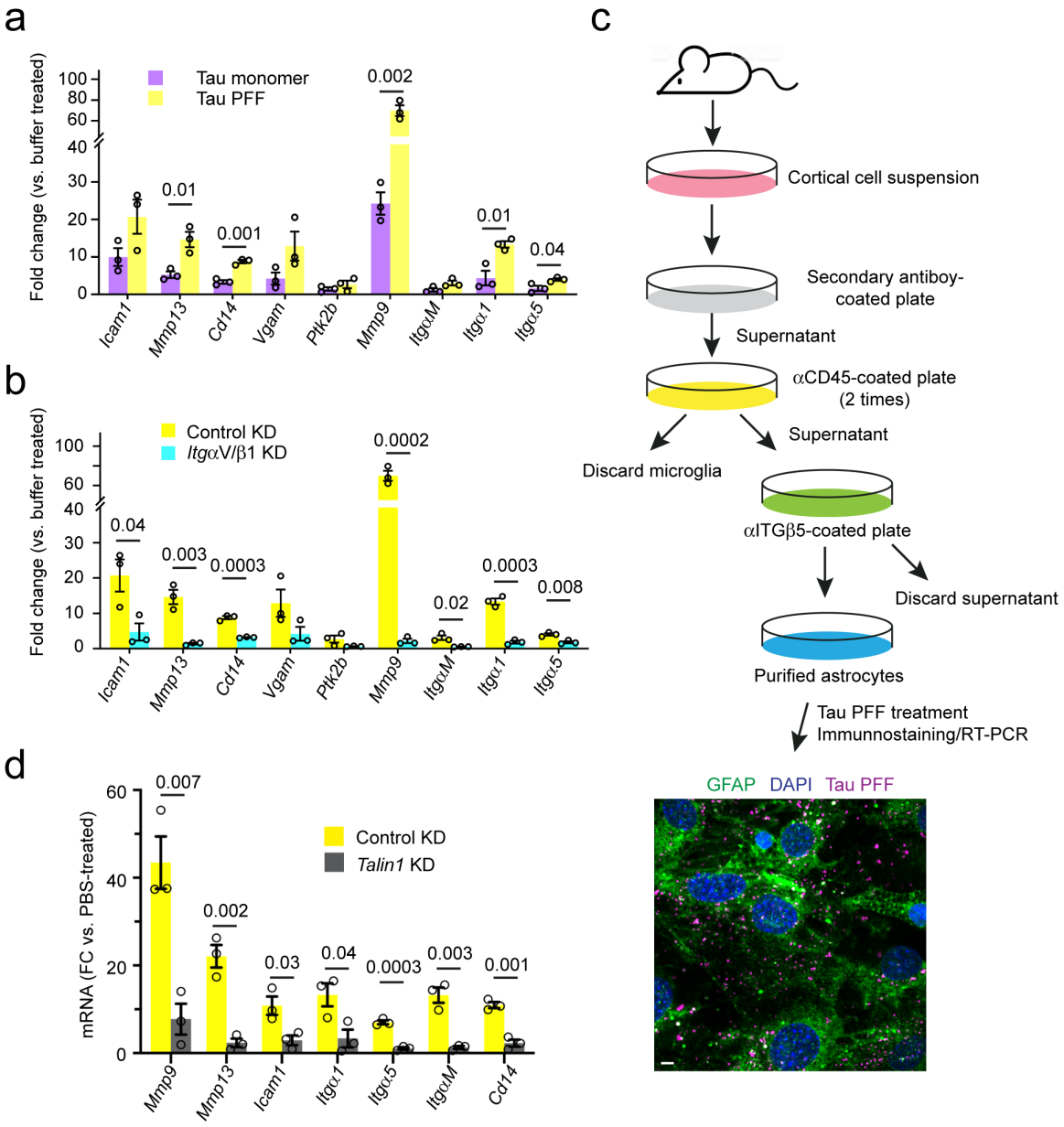
a
Fold change (vs. buffer treated)
Tau monomer
Tau PFF
0.002
0.01
0.001
0.01
0.04
Icam1
Mmp13
Cd14
Vgam
Ptk2b
Mmp9
ItgαM
Itgα1
Itgα5
b
Control KD
ItgαV/β1 KD
0.0002
0.04
0.003
0.0003
0.02
0.0003
0.008
c
Cortical cell suspension
Secondary antiboy-coated plate
Supernatant
αCD45-coated plate (2 times)
Supernatant
Discard microglia
αITGβ5-coated plate
Discard supernatant
Purified astrocytes
Tau PFF treatment
Immunnostaining/RT-PCR
GFAP DAPI Tau PFF
d
mRNA (FC vs. PBS-treated)
Control KD
Talin1 KD
0.007
0.002
0.03
0.04
0.0003
0.003
0.001
Mmp9
Mmp13
Icam1
Itgα1
Itgα5
ItgαM
Cd14

Figure 4

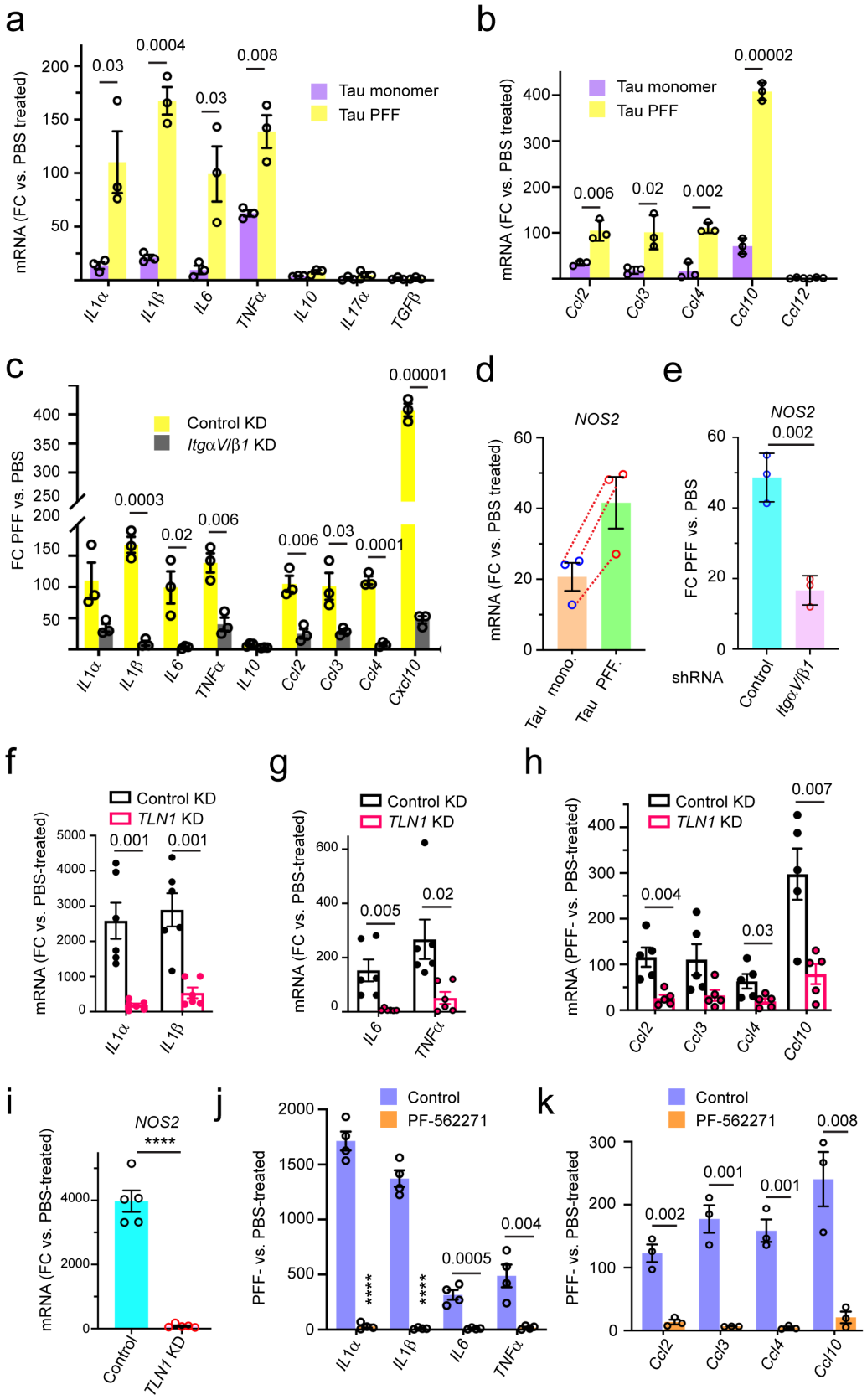
a
mRNA (FC vs. PBS treated)
Tau monomer
Tau PFF
0.03
0.0004
0.03
0.008
IL1α
IL1β
IL6
TNFα
IL10
IL17α
TGFβ
b
mRNA (FC vs. PBS treated)
Tau monomer
Tau PFF
0.006
0.02
0.002
0.00002
Ccl2
Ccl3
Ccl4
Ccl10
Ccl12
c
FC PFF vs. PBS
Control KD
ItgαV/β1 KD
0.0003
0.02
0.006
0.006
0.03
0.0001
0.00001
IL1α
IL1β
IL6
TNFα
IL10
Ccl2
Ccl3
Ccl4
Cxcl10
d
NOS2
mRNA (FC vs. PBS treated)
Tau mono.
Tau PFF.
e
NOS2
0.002
FC PFF vs. PBS
shRNA
Control
ItgαV/β1
f
Control KD
TLN1 KD
mRNA (FC vs. PBS-treated)
0.001
0.001
IL1α
IL1β
g
Control KD
TLN1 KD
mRNA (FC vs. PBS-treated)
0.005
0.02
IL6
TNFα
h
Control KD
TLN1 KD
mRNA (PFF- vs. PBS-treated)
0.004
0.03
0.007
Ccl2
Ccl3
Ccl4
Ccl10
i
NOS2
****
mRNA (FC vs. PBS-treated)
Control
TLN1 KD
j
Control
PF-562271
PFF- vs. PBS-treated
****
****
0.0005
0.004
IL1α
IL1β
IL6
TNFα
k
Control
PF-562271
PFF- vs. PBS-treated
0.002
0.001
0.001
0.008
Ccl2
Ccl3
Ccl4
Ccl10

Figure 5

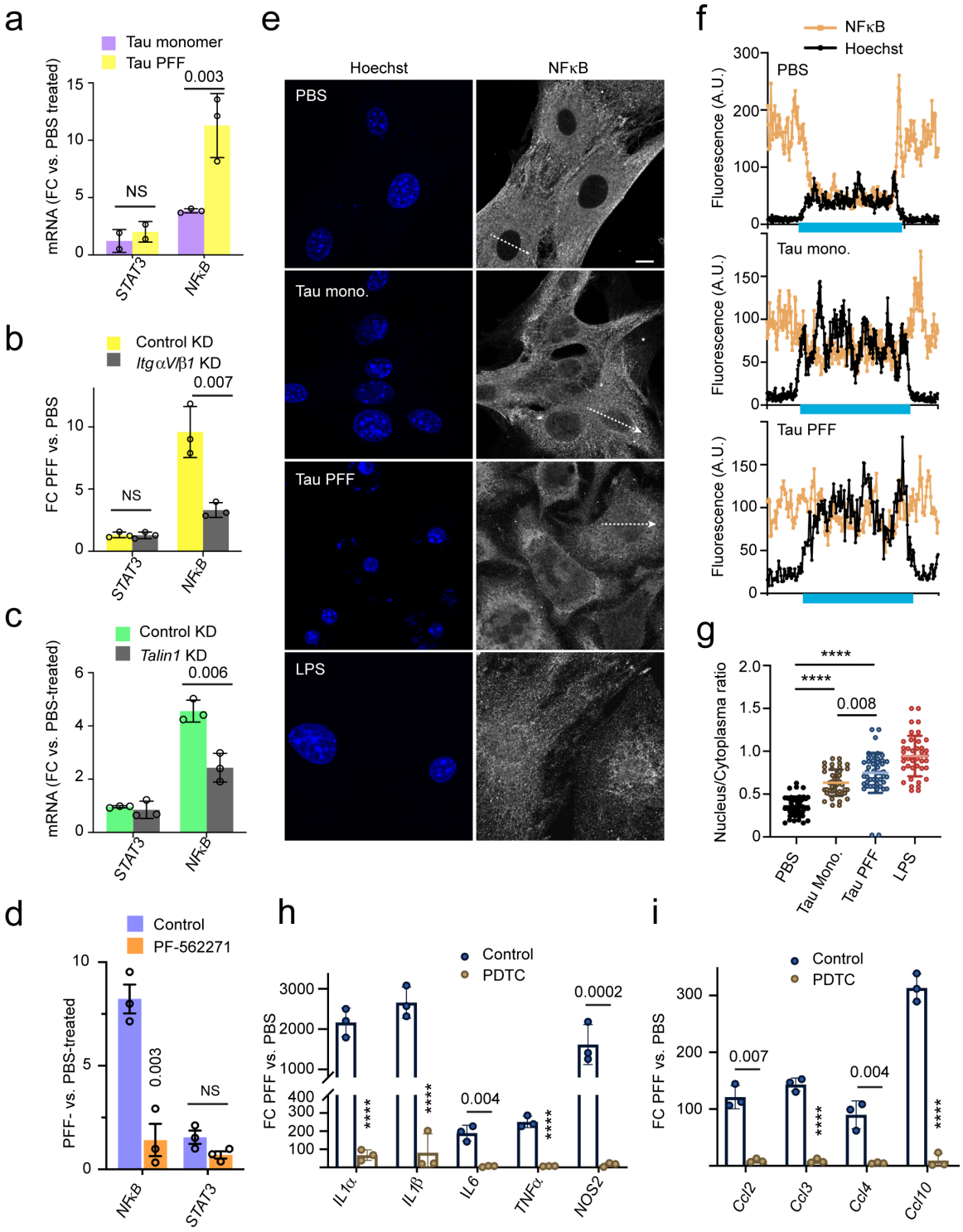
a
Tau monomer
Tau PFF
mRNA (FC vs. PBS treated)
0.003
NS
STAT3
NFκB
b
Control KD
ItgαV/β1 KD
FC PFF vs. PBS
0.007
NS
STAT3
NFκB
c
Control KD
Talin1 KD
mRNA (FC vs. PBS-treated)
0.006
STAT3
NFκB
d
Control
PF-562271
PFF- vs. PBS-treated
0.003
NS
NFκB
STAT3
e
Hoechst
NFκB
PBS
Tau mono.
Tau PFF
LPS
f
NFκB
Hoechst
PBS
Tau mono.
Tau PFF
Fluorescence (A.U.)
g
Nucleus/Cytoplasma ratio
****
****
0.008
PBS
Tau Mono.
Tau PFF
LPS
h
Control
PDTC
FC PFF vs. PBS
0.0002
0.004
****
IL1α
IL1β
IL6
TNFα
NOS2
i
Control
PDTC
FC PFF vs. PBS
0.007
0.004
Ccl2
Ccl3
Ccl4
Ccl10

Figure 6

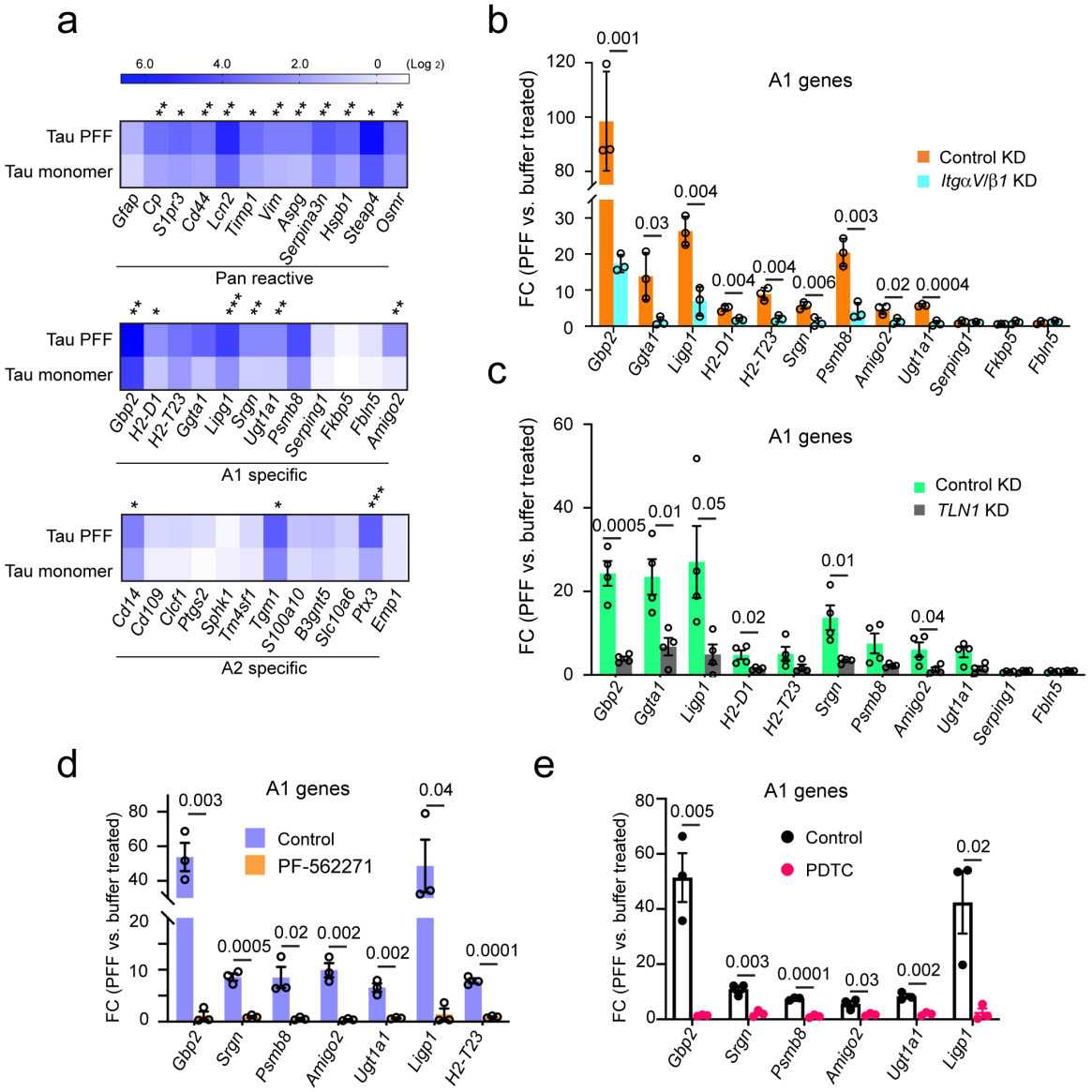
a
6.0
4.0
2.0
0
(Log 2)
Tau PFF
Tau monomer
Gfap
Cp
S1pr3
Cd44
Lcn2
Timp1
Vim
Aspg
Serpina3n
Hspb1
Steap4
Osmr
Pan reactive
Gbp2
H2-D1
H2-T23
Ggta1
Lipg1
Srgn
Ugt1a1
Psmb8
Serping1
Fkbp5
Fbln5
Amigo2
A1 specific
Cd14
Cd109
Clcf1
Ptgs2
Sphk1
Tm4sf1
Tgm1
S100a10
B3gnt5
Slc10a6
Ptx3
Emp1
A2 specific
b
A1 genes
Control KD
ItgαV/β1 KD
FC (PFF vs. buffer treated)
0.001
0.03
0.004
0.004
0.004
0.006
0.003
0.02
0.0004
c
A1 genes
Control KD
TLN1 KD
FC (PFF vs. buffer treated)
0.0005
0.01
0.05
0.02
0.01
0.04
d
A1 genes
Control
PF-562271
FC (PFF vs. buffer treated)
0.003
0.0005
0.02
0.002
0.002
0.04
0.0001
e
A1 genes
Control
PDTC
FC (PFF vs. buffer treated)
0.005
0.003
0.0001
0.03
0.002
0.02

Figure 7

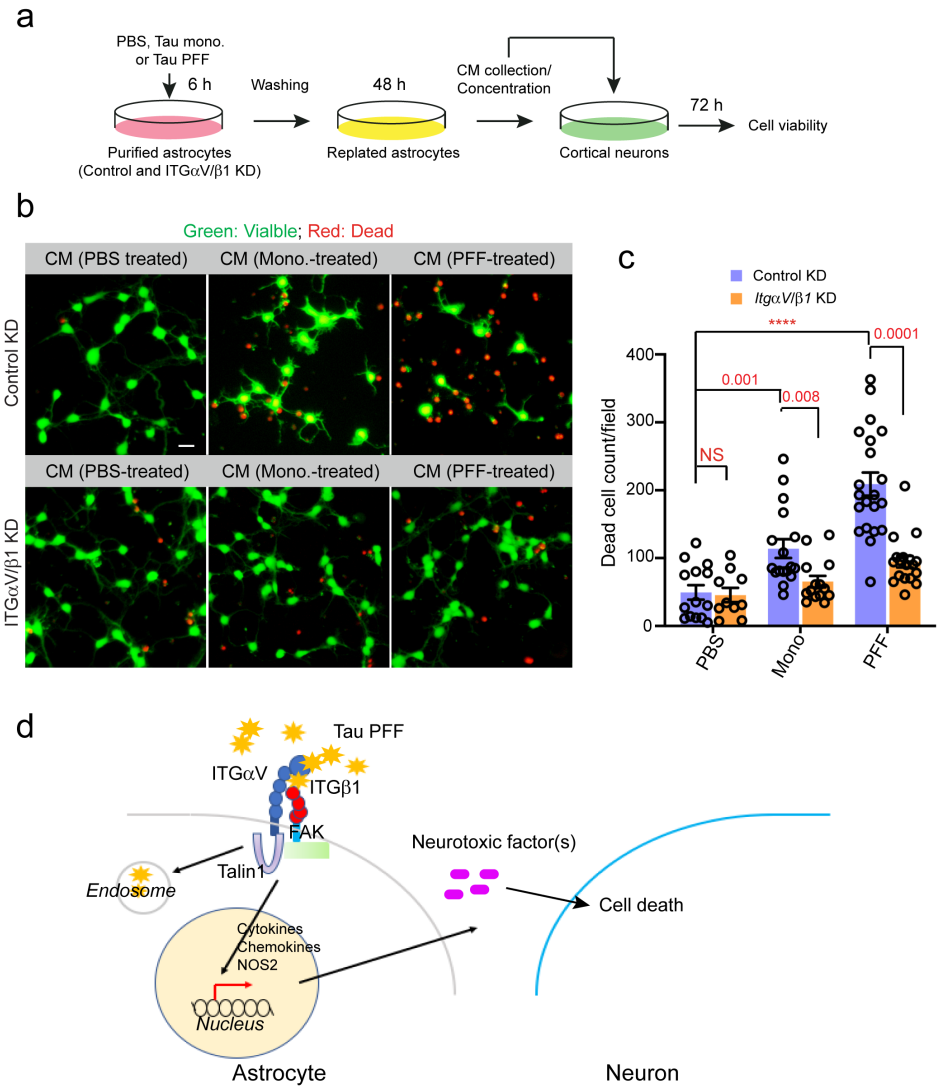
a
PBS, Tau mono.
or Tau PFF
6 h
Washing
48 h
CM collection/
Concentration
72 h
Cell viability
Purified astrocytes
(Control and ITGαV/β1 KD)
Replated astrocytes
Cortical neurons
b
Green: Vialble; Red: Dead
CM (PBS treated)
CM (Mono.-treated)
CM (PFF-treated)
Control KD
CM (PBS-treated)
CM (Mono.-treated)
CM (PFF-treated)
ITGαV/β1 KD
c
Control KD
Itgα V/β1 KD
****
0.0001
0.001
0.008
NS
Dead cell count/field
400
300
200
100
0
PBS
Mono
PFF
d
Tau PFF
ITGαV
ITGβ1
FAK
Talin1
Endosome
Cytokines
Chemokines
NOS2
Nucleus
Neurotoxic factor(s)
Cell death
Astrocyte
Neuron